JURNAL SAINS MATERI INDONESIA (JUSAMI)
ISSN: 1411-1098 (print), 2614-087X (online)
VOL. 23, ISSUE 2, April 2022
DOI: https://doi.org/10.17146/jsmi.2022.23.5.6356

ORIGINAL ARTICLE

Application of Rietveld Analysis to the Multiphase Crystal Structure of $Bi_{1/2}K_{1/2}TiO_3$ Using Molten Salt Synthesis

S. Ahda[1,*], A. Taufiq[1], Mardiyanto[1], A. Mahyudin[2] and E. Sukirman[1]

[1] Research Center for Nuclear Reactor Technology, National Research and Innovation Agency
[2] Physics Departement, Andalas University

ABSTRACT – Recently, an interesting application development of piezoelectric materials is as part of the tool for in-situ testing of nuclear fuel and the supporting materials in nuclear reactor, as well as sensors for safety systems in the reactor environment itself. One of the piezoelectric materials (lead free) is bismuth potassium titanate $Bi_{1/2}K_{1/2}TiO_3$ (BKT) which is used in this research and has been successfully synthesized using the molten salt method. This method is a simple process that reacts to the base material in a solution of NaCl and KCl salts to produce nanocrystal ceramics powder with good compositional homogeneity and sinterability. The synthesis process has been carried out in two stages, first to produce $Bi_2Ti_4O_{11}$ and then to add excess K_2CO_3 as a base material to produce BKT. The weight ratio between $Bi_2Ti_4O_{11}$ and excess K_2CO_3 was 1:1.5 and 1:2. Structural identification of the synthesized results has been done by Rietveld analysis of the XRD pattern using PAN-Analytical Highscore software. The multiphase of BKT has been obtained by a predominantly tetragonal crystal system, in addition to cubic as second phase. This is indicated by the content of the tetragonal and cubic phases obtained at 64.5 and 36.5% for the ratio 1:1.5 and 80.3 % and 19.7 % for the ratio 1:2, respectively.The addition of excess K_2CO_3 increases, the content of the tetragonal BKT phase increases. . Besides that, the “a” lattice parameter increases and the “b” lattice parameter decreases, if the K_2CO_3 content is added. Likewise, the size of the crystallite and microstrain decreases with the in excess K_2CO_3.

ARTICLE HISTORY
Received: 8 June 2021
Revised: 9 May 2022
Accepted: 9 May 2022

KEYWORDS
Molten salt method,
Williamson-Hall plot,
Piezoelectric

INTRODUCTION

Generally, measurements of nuclear fuel and material properties during irradiation are performed on samples at the end of the test, which results in errors due to handling and because measurements are not made under the pressure, flux, and/or high temperature of the nuclear fuel of the prototype. Therefore, the researchers began to develop real-time data measurement with in-situ instruments related to the phenomenon of nuclear fuel performance by using high-temperature piezoelectric materials as sensors. Such sensors can only provide information about the integral neutron effect or peak temperature. In-situ instrumentation in irradiation tests can provide real physical analysis, thereby showing the evolution of certain phenomena over time [1].

Selection of the performance of the piezoelectric material to be applicable and working under test conditions during irradiation, it is indicated by the value of the curie temperature (Tc) and the piezoelectric constant (d33). Pb-based (toxic) piezoelectric materials for Lead zirconate titanate $PbZr_xTi_{(1-x)}O_3$ (PZT) still dominate high-performance materials in a wide range of applications. Many researchers have tried to find other environmentally friendly alternative materials such as bismuth and barium-based piezoelectric [2]–[4]. The Pb-free materials are still being developed to replace PZT such as barium titanate $BaTiO_3$ (BT), bismuth sodium titanate $Bi_{1/2}Na_{1/2}TiO_3$ (BNT) or bismuth s titanate $Bi_{1/2}K_{1/2}TiO_3$ (BKT).

At the beginning of the application study, BT was also used as a potential candidate although it did not have a high piezoelectric constant. However the usefulness of BT has been limited as the low working temperature range of BT ceramics due to its low curie temperature (Tc = 120^{o}C). Likewise, BNT has been studied for a long time as a promising alternative with a high temperature curie (Tc = 320^{o}C) with a piezoelectric constant of 73 pC/N. Meanwhile, BKT has a relatively high Tc of 380 ^{o}C with d33 = 101 pC/N, and shows a better piezoelectric response than BNT and BT. But BKT has been studied much less than BNT material because of its weakness for preparing high density ceramics [5].

Therefore, Morozov [6] in his research showed that BKT has good piezoelectric properties. However, there are very few research reports on pure BKT. Synthesis of pure high-density BKT ceramics is relatively difficult due to the high volatility of the potassium component at the sintering temperature [7]–[9]. So this problem makes it limited in researching solid solution systems based on BKT. Therefore, this system needs to be studied more deeply.

BKT is a ferroelectric material having a typical perovskite structure with a tetragonal crystal system at room temperature[10], [11]. Recently, fabrication using the hot-pressing method, as practiced by Hiruma [8], has sintered at 1060°C and 1080°C and obtained the structure's single-phase perovskite. This is also difficult in fabrication using ordinary combustion techniques.

***CORRESPONDING AUTHOR** | S. Ahda | ✉ idnafahda@gmail.com

In this study, we report the synthesis of BKT nanocrystal ceramics by reacting basic materials in NaCl + KCl salt solution, named by the molten salt method. The synthesis has been carried out in two stages, namely synthesizing $Bi_2Ti_4O_{11}$ first and then producing BKT. This study aims to determine the effect of excess K_2CO_3 added to $Bi_2Ti_4O_{11}$ to obtain a tetragonal perovskite BKT structure as the main phase, in addition to cubic BKT as the second phase.

The results of the synthesis were characterized using the XRD technique and continued with Rieltveld analysis for the synthesis of multi-phase BKT using the molten salt method. The use of the Highscore program to refine the xrd data becomes very useful in identifying changes in the crystal system and the content of the phases.

EXPERIMENTAL METHOD

That As one of the objectives of this study is the synthesis of BKT powder using the molten salt method [12]–[14]. The synthesis of bkt using this method is the reaction of basic materials to form synthesis products in a molten salt environment. The product itself can be separated by washing with boiling water The synthesis of BKT has been carried out in two stages, starting with the synthesis of $Bi_2Ti_4O_{11}$ (BTO) and then BKT This same technique with two stages has also been applied by P. Setasuwon for the synthesis of BNT materials [15].

Metal oxide or carbonate powders from Bi_2O_3 (99.999%, ABCR), TiO_2 (99.99%, STREAM) and K_2CO_3 (99.998%, ABCR) with reagent content were used as the base material. The base material mixture between Bi_2O_3 and TiO_2 can be expected to become $Bi_2Ti_4O_{11}$ (BTO) as a result of the first stage reaction then followed by the addition of n K_2CO_3 to produce CO_2 products, (n-1) K_2CO_3 and BKT as the second stage reaction.

For the synthesis of BTO and BKT, each mixture of basic materials was added with NaCl and KCl salts (with a mole ratio of 1:1). The weight ratio between the mixture and salt was 1:1, then continued mixing and grinding mechanically using agate mortar for 4 hours. To obtain two variations of BKT synthesized samples, the BTO content was reacted with excess K_2CO_3 with a weight ratio between BTO and K_2CO_3 of 1:1.5 and 1:2, respectively.

In this molten salt synthesis study, the BTO samples were sintered at 950°C for 4 hours, while the BKT samples were at 650°C for 5 hours. Na^+ ,K^+ salts and unreaction K_2CO_3 residue can be removed by washing using boiling water many times. The absence of salt can be checked with a drop of $AgNO_3$ solution

The characterization of the synthesis results has also been carried out using x-ray diffraction, in order to obtain the form of the reaction product compounds and crystal structure analysis.

RESULT AND DISCUSSION

Regarding the manufacture of piezoelectric ceramic powder, the molten salt technique is an easier and more practical way when compared to conventional techniques (solid state reaction) which require high temperatures (1000–1300°C) [16], [17]. The diffuse reactions between Bi, K, Ti and O occur in this molten salt technique facilitated in liquid salt to obtain BTO or BKT precursors. As mentioned above, the BTO intermediate product synthesis has been carried out before the BKT synthesis process. The BTO products was clarified by X-Ray Diffraction (XRD) as shown in Figure 1.

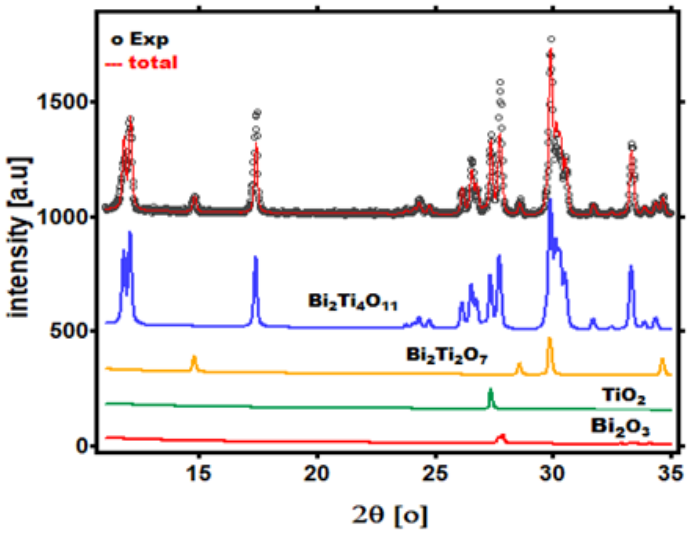

Figure 1. X-ray diffraction pattern from the synthesis product for the mixed reaction of BiO_2 and TiO_2 and then refinement is carried out. The intensity of the experimental data is labeled o (black circle marker) and the total calculation is labeled - (red line)

The XRD patterns of the Bi_2O_3 and TiO_2 reaction results to produce BTO were identified using Rietveld method [18] by the HighScore PAN-Analytical software [19] (a PW1710 type PANanalytical EMPYREAN) through the refinement process, so that the compounds formed could be identified. The initial refinement was done by inputting the zero-point shift, background, machine parameters and the unit-cell parameters. The XRD peak positions were more identical to the synthesis carried out by P. Sutawasun at 1100°C by obtaining the $Bi_2Ti_4O_{11}$ compound [15]. This makes $Bi_2Ti_4O_{11}$ (ICSD collection code: 79768) used as one of the input parameters of the refinement, in addition to $Bi_2Ti_2O_7$ (ICSD collection code: 161101). The results of the refinement process are identical to the statistical value of the goodness of fit of 2.45.

As a result of refnement, the contents of the synthesis product of $Bi_2Ti_4O_{11}$, $Bi_2Ti_2O_7$ and the base material of TiO_2 and BiO_2 (still present) were obtained at 90.8, 7.8, 0.8 and 0.6%, respectively, as shown in Figure 1. Indication of the peaks of the $Bi_2Ti_2O_7$ compound was shown more clearly at an angle of 14.78 and 28.62°. So in other words, the synthesis product using the molten salt method at a sintering temperature of 950°C has been successfully carried out, which can be shown predominantly by the compounds of $Bi_2Ti_4O_{11}$ and $Bi_2Ti_2O_7$.

The dominant $Bi_2Ti_4O_{11}$ powder phase was mixed with various K_2CO_3 (weight ratio between $Bi_2Ti_4O_{11}$ and K_2CO_3 materials are 1:1.5 and 1:2) into NaCl + KCl powder and continued with sintering at a low temperature of 650°C as shown in the XRD pattern by Figure 2. Conversion of $Bi_2Ti_4O_{11}$ to $Bi_{1/2}K_{1/2}TiO_3$ has occurred at a low temperature of 650°C. It is expected that the low energy diffusion conversion of K ions to $Bi_2Ti_4O_{11}$ can form $Bi_{1/2}K_{1/2}TiO_3$.

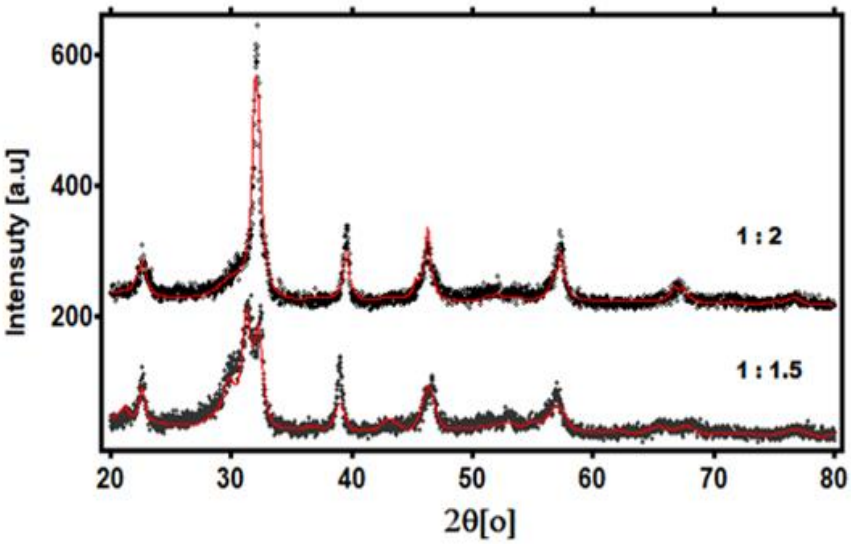

Figure 2. XRD pattern of $Bi_{1/2}K_{1/2}TiO_3$ (black dot) with the addition of K_2CO_3 (ratio of 1:1.5 and 1:2) and the total calculation pattern from the refinement result (red line) using two phases (teragonal and cubic)

Figure 2 illustrates the XRD diffraction pattern of two phases of BKT synthesis products with the basic material weight ratio between $Bi_2Ti_4O_{11}$ and K_2CO_3 of 1:1.5 and 1:2, respectively. The two patterns have a slightly different profile, especially at the diffraction angle range (2 theta) of 25–35°, although the existence of identical peaks is the same. The crystal system of $Bi_{1/2}K_{1/2}TiO_3$ has two types of perovskite structures, namely tetragonal and cubic. These two types have also been inputted into the refinement process with a tetragonal crystal system (ICSD code 98-009-8057), and cubic (ICSD code 98-010-9151). the tetragonal phase peaks for the planes (110) and (011) shift are closer together for the 1:2 ratio. The cubic peaks (represented by the plane (011)) shown at the peak around of 30° are broader and lower, while the tetragonal peaks (011) and (110) planes shown at the 30.5–33.5° angle range are higher and sharper, if the content K_2CO_3 is added, as shown in Figure 3, the tetragonal phase peaks for the planes 110 and 011 shift are closer together for the 1:2 ratio. This has indicated a change in crystal shape, so that changes in the lattice parameters themselves have occurred, as supported in the refinement results (Table 1) The two phases with the perovskite crystal structure contributed quite well in the refinement, so that the XRD pattern showed no unknown peak, except at an angle of 18° in the ratio 1:1.5.

The results of this refinement can be seen in Table 1, the statistical error of the refining process shown by R_{wp} (less than 22%) and R_{exp} (less than 16%) is still low, as explained by Toby [20]. Meanwhile, the value of goodness of fit is still below 1.963. This is also supported by the refinement results for the cubic phase content decreases from 35.5 to 19.7% and the tetragonal phase content to increase from 64.5 to 80.3%.

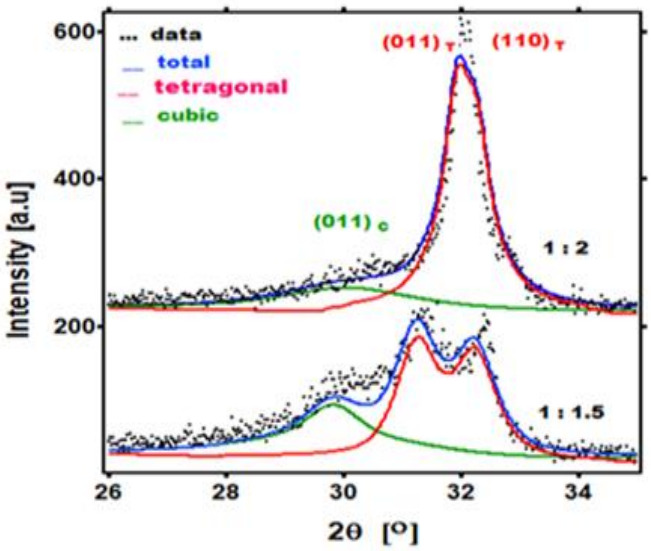

Figure 3. Refinement XRD pattern of $Bi_{1/2}K_{1/2}TiO_3$ (with a ratio of 1:1.5 or 1:2) at an angle range of 25–35° for tetragonal (red line) and cubic (green line) structures. The dots represent the intensity of experimental data, the blue line represents the total intensity calculation.

Table 1. The results of the refinement process for samples with a weight ratio of between the $Bi_2Ti_4O_{11}$ and K_2CO_3 mixture of 1:1.5 and 1:2

Refinement Results	1 :1.5	1:2
Goodness of Fit	1.755	1.963
R (expected), Rexp [%]	15.375	16.061
R(weighted profile), Rwp [%]	20.369	22.501
Tetragonal		
Spacegroup P4mm		
Weight fraction [%]	64.5	80.3
Lattice pameters: a [A]	3.9054	3.9285
b [A]	4.1572	4,0096
Cubic		
Spacegroup P-3mm		
Weight fraction [%]	35.5	19.7
Lattice pameters: a [A]	4.2138	4.2101

Due to the change in the addition of K_2CO_3 content in the salt solution at a low sintering temperature of 650°C for 5 hours, it is possible that the reaction is not complete. This can be seen from the presence of cubic BKT content that still exists. Therefore, crystal imperfections can cause differences in crystallite size and micro-strain, however using the Williamson-Hall equation to analyze the XRD pattern is more precise than using the Scherrer equation [21], [22].

The full width at half maximum (FWHM) of the experimental XRD peaks was modeled to a Gaussian form. The actual broadening (β) of the diffraction pattern is corrected for the experimental broadening (β_{ex}) and the instrumental broadening (β_{in}) as $\beta_2 = \beta_{ex2} - \beta_{in2}$, corresponding to each diffraction peak of BKT Due to the influence of the size and effect of the strain, the Williamson-Hall equation [18] can be modeled from the actual broadening as a result of the corrected refinement as follows:

$$\beta = (K\lambda/D \cos\theta) + 4\varepsilon \tan\theta \quad (1)$$

where $(K\lambda/D \cos\theta)$ is broadening due to the size (D) and $4\varepsilon \tan\theta$ is broadening due to strain (ε). The modification of equation (1) yields,

$$\beta \cos\theta = (K\lambda/D) + 4\varepsilon \sin\theta \quad (2)$$

where β is the full width at half maximum of the XRD peaks, θ is the position of the peaks, K is the Debye–Scherrer constant (0.94 for spherical nanoparticles) , λ = 1.5404 Angstroom is the x-ray wavelength. Equation 2 is used to plot the

graph of β cosθ verses sinθ and is fitted with linear regression for the data as shown in Figure 4. The inverse of the intercept on the y-axis at x = 0 gives the crystallite size (D) and the slope of the fit gives the strain (ε).

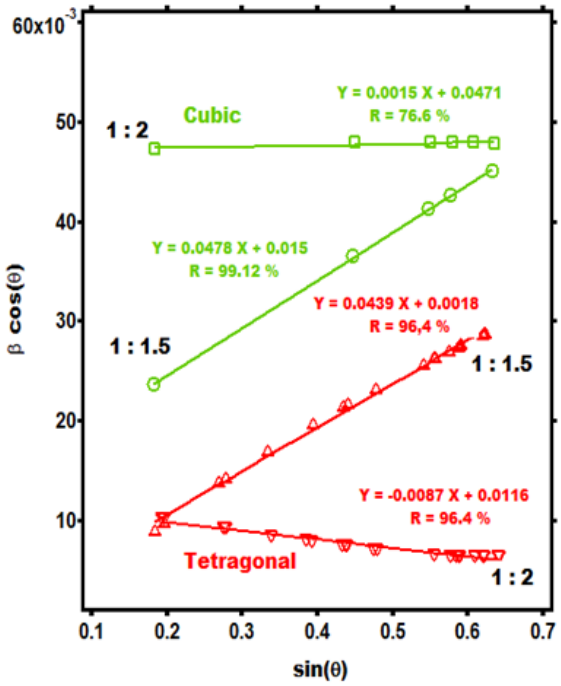

Figure 4. Wilamson-Hall plots of the tetragonal and cubic phases for the addition of K_2CO_3 ratio (1:1.5 and 1:2), respectively and the linear regression equation and the statistical R square value

The size of the nanocrystalline BKT for a ratio of 1:1.5 (between the base material content of BTO with the addition of K_2CO_3) and 1:2 can be determined by the Wilamson Hall plot approach [17], as shown in Figure 4. The tetragonal and cubic phases of BKT show small variations in the dimensions of due to displacement of the atomic position for each addition of K^2CO_3. The crystallite and microstrain sizes determined from the W-H equation have been calculated and tabulated in Table 2.

Table 2. The microstructure parameters on the crystal size (D) of the microstrain (ε) changed with the addition of K_2CO_3

	Ratio	D [nm]	ε
Tetragonal	1:1.5	80.443	$1.097\ 10^{-2}$
	1:2	12.482	$-2.17\ 10^{-3}$
Cubic	1:1.5	9.6531	$1.19\ 10^{-2}$
	1:2	3.0742	$3.75\ 10^{-4}$

Especially for the 1:2 ratio, the negative slope of the tetragonal phase shows that the microstrain that occurs in the crystal does not have a dominant effect on the broadening of the peaks, as explained for the BaF_2 sample by Langford [23], [24].

It was found that the tetragonal and cubic phases were retained in their structure by the addition of K_2CO_3, even with slight changes. In other words, the crystallite and microstrain also decreased with the addition of K_2CO_3. But the two types of phases also have small variations in dimension due to the displacement of the atoms in the unit cell, as shown in Table 2.

The effect of excess K_2CO_3 added to $Bi_2Ti_4O_{11}$ produces BKT with two phases (tetragonal and cubic), as well as changes in crystallite size and micro strain.

CONCLUSION

Synthesis of BKT using the molten salt method has been successfully carried out in two stages, starting with BTO synthesis at a sintering temperature of 950°C for 4 hours and then continued by BKT synthesis at 650°C for 5 hours, as the final product. The effect of excess K_2CO_3 addition in BKT synthesis has been successfully identified and characterized using multiphase Rietveld analysis of the XRD pattern for both stages. The addition of excess K_2CO_3 to BTO has been able to affect the formation of BKT compounds with perovskite crystal systems, both tetragonal and cubic. The content of tetragonal (dominant) and cubic phases was obtained 64.5 and 35.5% for the ratio of BTO and K_2CO_3 of 1: 1.5, and also 80.5 and 19.5% for the ratio of 1: 2, respectively. The largest crystallite size as the tetragonal phase was obtained 80.443 nm on a ratio of 1: 1.5, while the lowest mcrostrain was obtained $3.75x10^{-4}$ from the cubic phase.

ACKNOWLEDGEMENT

I thank Mr. Iman Kuntoro as the former director of the PSTBM-BATAN has given permission to carry out this research, both the program and the use of the current budget at that time. Besides that, me and Mr. Imam Kuntoro has had frequent scientific discussions about this research and its applications. I give thanks for Dr. Abu Khalid as the head of BSBM-PSBM for discussion and administrative permission from our institution, as well as for Miss. Iin Lidia who has supported various technical implementations in the laboratory.

REFERENCES

[1] B. T. Reinhardt, A. Suprock, and B. Tittmann, "Testing piezoelectric sensors in a nuclear reactor environment", *AIP Conf. Proc.*, vol. 1806, 2017.
[2] J. Rödel, W. Jo, K. T. P. Seifert, E. M. Anton, T. Granzow, and D. Damjanovic, "Perspective on the development of lead-free piezoceramics", *J. Am. Ceram. Soc.*, vol. 92, no. 6, pp. 1153–1177, 2009.
[3] Y. Zhang, V. Y. Topolov, A. N. Isaeva, C. R. Bowen, H. Pearce, and H. Khanbareh, "Lead-free relaxor-like $0.75Bi_{0.5}K_{0.5}TiO_3$ - $0.25BiFeO_3$ Ceramics with large electric field-induced strain", *2019 IOP Publ. Ltd, Smart Mater. Struct.*, vol. 28, no. 12, 2019.
[4] T. R. Shrout and S. J. Zhang, "Lead-free piezoelectric ceramics: Alternatives for PZT?", *J. Electroceramics*, vol. 19, no. 1, pp. 111–124, 2007.
[5] E. D. Pinheiro and T. Deivarajan, "A concise review encircling lead free porous piezoelectric ceramics", *Acta Phys. Pol. A*, vol. 136, no. 3, pp. 555–565, 2019.
[6] M. I. Morozov, M. A. Einarsrud, T. Grande, and D. Damjanovic, "Lead-free relaxor-like $0.75Bi_{0.5}K_{0.5}TiO_3$ - $0.25BiFeO_3$ Ceramics with large electric field-induced strain", *Ferroelectrics*, vol. 439, no. 1, pp. 88–94, 2012.
[7] T. Wada, A. Fukui, and Y. Matsuo, "Preparation of $(K_{0.5}Bi_{0.5})TiO_3$ ceramics by polymerized complex method and their properties", *Japanese J. Appl. Physics, Part 1 Regul. Pap. Short Notes Rev. Pap.*, vol. 41, no. 11 B, pp. 7025–7028, 2002.
[8] Y. Hlruma, H. Nagata, and T. Takenaka, "Grain-size effect on electrical properties of $(Bi_{1/2}K_{1/2})TiO_3$ ceramics", *Japanese J. Appl. Physics, Part 1 Regul. Pap. Short Notes Rev. Pap.*, vol. 46, no. 3 A, pp. 1081–1084, 2007.
[9] M. HAGIWARA, "(Bi1/2K1/2)TiO3 lead-free ferroelectric ceramics: processing, properties, and compositional modifications", *J. Ceram. Soc. Japan*, vol. 129, no. 8, pp. 496–503, 2021.
[10] C. F. Buhret, "Some properties of bismuth perovskites", *J. Chem. Phys.*, vol. 36, no. 3, pp. 798–803, 1962.
[11] Y. Kitanaka, Y. Noguchi, and M. Miyayama, "Uncovering ferroelectric polarization in tetragonal $(Bi_{1/2}K_{1/2})TiO_3$–$(Bi_{1/2}Na_{1/2})TiO_3$ single crystals", *Sci. Rep.*, vol. 9, no. 1, pp. 1–8, 2019.
[12] S. Ahda, S. Misfadhila, P.Parikin, and T. Y. S. P. Putra, "Molten Salt Synthesis and Structural Characterization of $BaTiO_3$ Nanocrystal Ceramics", *Int. Conf. Adv. Mater. Better Futur. 2016 , Ser. Mater. Sci. Eng.*, vol. 176, no. 1, 2017.
[13] S. Park *et al.*, "An easy approach to obtain textured microstructure and transparent seed crystal prepared by simple molten salt synthesis in modified potassium sodium Niobate", *J. Eur. Ceram. Soc.*, vol. 40, no. 4, pp. 1232–1235, 2020.
[14] S. Ahda, Mardiyanto, A. Taufiq, and M. Silalahi, "The Synthesis of $PbZr_{0.52}Ti_{0.48}O_3$ and $PbZr_{0.58}Ti_{0.42}O_3$ Ceramic Powder by Use Molten Salt Method and Its Intermediate Product Analysis", *Maj. Ilm. Pengkaj. Ind.*, vol. 13, no. 3, p. 195, 2019.
[15] P. Setasuwon, N. Vaneesorn, S. Kijamnajsuk, and A. Thanaboonsombut, "Nanocrystallization of $Bi_{0.5}Na_{0.5}TiO_3$ piezoelectric material", *Sci. Technol. Adv. Mater.*, vol. 6, no. 3–4 SPEC. ISS., pp. 278–281, 2005.
[16] M. Hagiwara, M. Ito, and S. Fujihara, "Defects and microstructure of a hydrothermally derived $(Bi_{1/2}K_{1/2})TiO_3$ powder", *J. Asian Ceram. Soc.*, vol. 5, no. 1, pp. 31–35, 2017.
[17] R. Sumang, C. Kornphom, and T. Bongkarn, "Synthesis and electrical properties of BNT-BKT-KNN lead free piezoelectric solid solution prepared via the combustion technique", *Ferroelectrics*, vol. 518, no. 1, pp. 11–22, 2017.
[18] P. Zhao, L. Lu, X. Liu, A. G. D. la Torre, and X. Cheng, *Error Analysis and Correction for Quantitative Phase Analysis Based on Rietveld-Internal Standard Method: Whether the Minor Phases Can Be Ignored?, Special Issue MPDPI Editor Igor Djerdj*. r Basel, Switzerland, 2019.

[19] J. Kaur, S. K. Tripathi, Ankush, M. D. Sharma, Kanika, and N. Goyal, "Rietveld Refinement Study of $GeSb_2Te_4$ Bulks Prepared Through Distinct Melting Profiles", *Mater. Today Proc.*, vol. 4, no. 9, pp. 9524–9528, 2017.
[20] B. H. Toby, " R factors in Rietveld analysis: How good is good enough?", *Powder Diffr.*, vol. 21, no. 1, pp. 67–70, 2006.
[21] A. A. Kadam, S. S. Shinde, S. P. Yadav, P. S. Patil, and K. Y. Rajpure, "Structural, morphological, electrical and magnetic properties of Dy doped Ni-Co substitutional spinel ferrite", *J. Magn. Magn. Mater.*, vol. 329, pp. 59–64, 2013.
[22] S. Sarkar and R. Das, "Determination of structural elements of synthesized silver nano-hexagon from X-ray diffraction analysis", *Indian J. Pure Appl. Phys.*, vol. 56, no. 10, pp. 765–772, 2018.
[23] J. I. Langford, R. J. Cernik, and D. Louer, "Breadth and shape of instrumental line profiles in high-resolution powder diffraction", *J. Appl. Crystallogr.*, vol. 24, no. pt 5, pp. 913–919, 1991.
[24] U. Zalilah and R. Mahmoodian, "Comparative study on microstructure, crystallite size and lattice strain of as-deposited and thermal treatment silver silicon nitride coating on Ti6Al4V alloy", *IOP Conf. Ser. Mater. Sci. Eng.*, vol. 210, no. 1, 2017.